

ORIGINAL RESEARCH PAPER

Photocatalytic Removal of Food Colorant E 131 VF from Synthetic Wastewater by Cu Doped TiO₂ Samples

M. El Tfayli¹, F. Makki¹, M. Kassir¹, M. El Jamal^{1,*}, A. Ebrahimian Pirbazari^{2,*}

¹ Chemistry Department, Lebanese University, Rafic Hariri Campus. El Hadath, Lebanon.

² Faculty of Fouman, College of Engineering, University of Tehran, Fouman, Iran.

Received: 2019-06-09

Accepted: 2019-07-16

Published: 2019-08-01

ABSTRACT

In this work, we studied the effect of various amounts (0.2-1.2 % mole ratio) of Cu doping to TiO₂ nanoparticles (Cu/TiO₂) on the photocatalytic removal efficiency of the food colorant E 131 VF. Two series of doped TiO₂ (P25) photocatalysts were prepared in two different media (50%ethanol-50%acetone and 5% surfactant (Tween 20)-95%H₂O) by using the impregnation method. The prepared samples were characterized by XRD, FTIR, Raman, diffuse reflectance spectroscopy and SEM/EDX analyses. The XRD results showed that the crystal dimension of TiO₂ increased from 23 to 35 nm and rutile/anatase ratio decreased from 16% to 9% after Cu doping in two different media. The photoactivity of TiO₂ was reduced in the presence of Cu even at a low molar ratio. The photocatalytic degradation rate constant of TiO₂ (P25) was 0.24 (au) but it decreased to 0.015 (au) in the presence of the sample containing 0.6% Cu. Several reasons were suggested to explain the dramatic decrease in the activity of the prepared Cu/TiO₂ samples.

Keywords: Cu/ TiO₂, Photocatalytic removal, Impregnation, Surfactant, and E 131 VF dye, Kinetics study

How to cite this article

El Tfayli M, Makki F, Kassir K, El Jamal M, Ebrahimian Pirbazari A. Photocatalytic Removal of Food Colorant E 131 VF from synthetic wastewater by Cu Doped TiO₂ Samples. J. Water Environ. Nanotechnol., 2019; 4(3): 187-197.
DOI: 10.22090/jwent.2019.03.002

INTRODUCTION

The food products may lead to numerous problems for human health because they are containing a number of harmful organic compounds. A number of studies have focused on the use of additives and their influence on humans and on the environment [1, 2]. The food colorants have been found large applications in food industry. An environmental regulation applied in most countries requires discoloring industrial wastewater prior to its discharge. A number of techniques for dyed wastewater purification based on biodegradation [3], electrochemical treatment [4, 5], adsorption [6], and advanced oxidation processes [7, 8] are suggested as solution to remediate this problem. There are some reports

about using photocatalytic degradation processes for the removal of dyes from wastewater [9–11]. Photocatalytic reactions based on semiconductor nanomaterials are started by absorption of radiation with energy that equals or higher than the band-gap energy of the catalyst. The absorption promotes an electron from the valence band (VB) of the photocatalyst to the conduction band (CB), thus generating a hole (h⁺) in the valence band [12]. TiO₂ has been found to be the most suitable and very researched material due to the high chemical stability and non-harmfulness, physical, optical and electrical properties [10, 13]. It exists in three phases: anatase, rutile, and brookite [13]. Anatase phase is mainly used as a photocatalyst but rutile phase has low catalytic activity [13]. Several efforts have been made to increase the photocatalytic efficiency

* Corresponding Author Email: mjamal@ul.edu.lb,
aebrahimian@ut.ac.ir



This work is licensed under the Creative Commons Attribution 4.0 International License.

To view a copy of this license, visit <http://creativecommons.org/licenses/by/4.0/>.

of TiO_2 , such as doping it with metal [14–20]. The photodegradation of methyl orange (MO) was increased after doping of TiO_2 with Cu [21]. Complete degradation of crystal violet (CV) was observed by Au doped TiO_2 , whereas for undoped TiO_2 was not observed [22]. The effect of metal ions on the photoactivity of TiO_2 has been investigated for degradation of organic pollutants [23–25]. Some studies have suggested that improvement of the photocatalytic degradation rate was due to electron trapping by the metal ions leading to the inhibition of electron-hole recombination. However, high concentration of metal may have a detrimental effect on the photoactivity of TiO_2 [24]. The nature of the metal and the dopant concentration have remarkable effect on the photocatalytic removal of the pollutant [25]. In contrast, some studies showed that the presence of some metals such as Fe(III) and Cr(III) in TiO_2 decreases the degradation rate constant of pollutants compared with pure TiO_2 [26]. The authors explained the dramatic decrease by a progressive loss of total crystallinity, partial transition from anatase to rutile phase. There are various experimental conditions that used for doped TiO_2 sample preparation and effect on photocatalytic activity, therefore experiments are necessary to point out these conditions on photocatalytic activity [15, 24, 27–28].

In this work, we prepared Cu doped TiO_2 (P25) containing different amounts of Cu in two different media for the degradation of the food colorant E 131 VF. The first set samples (1st procedure) were prepared in 50% ethanol- 50% acetone; another set (2nd procedure) were prepared in 5% surfactant (Tween 20) – 95 % water. The reason for using these two media was an attempt to overcome the nanoparticles agglomeration observed when using water alone as a solvent [29]. To the author's knowledge, use of two different media for the preparation of Cu doped TiO_2 samples and investigation of their performance for degradation of the food colorant E 131 VF has not been reported yet.

EXPERIMENTAL DETAILS

TiO_2 (P25) was provided from Degussa (Sigma Aldrich, Germany,) consists of 80% anatase and 20% rutile with a specific BET surface area of $50 \text{ m}^2 \text{ g}^{-1}$ and primary particle size of 23 nm. The food colorant, E131VF dye selected as an organic pollutant model, was purchased from Sigma Aldrich ($\text{C}_{27}\text{H}_{31}\text{N}_2\text{O}_6\text{S}_2\text{-Na}$, purity: 50 %, M_w : 565.67 g).

$\text{Cu}(\text{NO}_3)_2 \cdot 3\text{H}_2\text{O}$ was purchased from BDH (GPR).

Preparation of Cu doped TiO_2 samples

The impregnation method was selected to doping the metal according to the procedure in ref. [29]. Several masses of $\text{Cu}(\text{NO}_3)_2 \cdot 3\text{H}_2\text{O}$ (BDH, GPR) were added each time to 2 g of TiO_2 in order to have samples containing 0.2–1.2 % mole ratio of Cu(II)/TiO_2 , and then 100 ml of equal volume of ethanol and acetone were added to each sample and stirred with a magnetic stirrer for 8 h, at room temperature. The solutions were allowed to stand at room temperature for 12 h and dried at 100°C for another 12 h. The dried samples were ground in a mortar and annealed at 400°C for 4 h. In this impregnation method, the metal ion is deposited on the surface of TiO_2 [18]. Another set (2nd procedure) of the samples were also prepared with 100 ml of distilled water containing 5 ml of the surfactant Tween 20. 2 g of TiO_2 followed the same steps without the addition of metal ion in order to compare it with the doped catalyst (0 % Cu/TiO_2) was prepared. The prepared catalysts were named x% Cu, y, where x is the Cu/TiO_2 molar ratio and y is the medium where the impregnation was done. A stock solution of E 131 VF dye was prepared by dissolving 40 mg of the dye in 1000 ml distilled water. The concentration of the dye in the experiment was selected in such a way that the absorbance of the dye followed Beer's law.

Characterization

The X-ray diffraction patterns for crystallinity investigation were recorded on D8 Focus, Bruker, X-ray diffractometer operating at 50 kV using $\text{Cu-K}\alpha$ radiation ($\lambda = 0.1541 \text{ nm}$). The measurement was performed over a diffraction angle range of $2\theta = 10^\circ\text{--}80^\circ$. The % of the rutile phase in the samples was determined with the following equation (Eq. 1):

$$\text{Rutile (weight \%)} = \frac{1}{1 + 0.884 \times I_A / I_R} \quad (1)$$

Where I_A and I_R are the diffraction intensity of the anatase and rutile phases, respectively [30].

FTIR spectra of the samples were recorded on Jasco FT/IR- 6300 spectrometers in the wavenumber range of 400 to 4000 cm^{-1} for functional groups identification. The FTIR study was performed by using KBr pellet. Raman spectra for characterization of surface functional groups were recorded on Horiba Scientific, operating

with green Laser at 532 nm. Scanning electron microscopy (SEM) images for investigation of the morphology corresponding to the achieved specimens were taken with Ametek materials analysis division (AIS 2300C series) instrument (working distance: 25 mm, voltage 20 kV). The optical band gap energies of the prepared materials were determined by UV-Vis DRS technique using Jasco V-570 spectrophotometer.

Photocatalytic degradation tests

The degradation of the food colorant E 131 VF was followed by measuring the absorbance (A) at the maximum absorption wavelength of E 131 VF dye (640 nm) with time. UV- visible spectra were recorded on a double beam UV-visible spectrophotometer. The determination of the order of the degradation reaction and the rate constant (arbitrary unit (au)) were obtained from the curve A vs time. Prior to commencing illumination, a suspension containing 0.08 g of the catalyst and 100 ml of aqueous solution of E 131 VF dye was stirred continuously at least for 15 min in the dark (for adsorption/desorption equilibrium), then the

sample was irradiated under magnetic stirring by 4 UVB lamps (λ_{\max} : 360 nm) positioned at 10 cm above the glass bowl (Luzchem LZC-4V, Canada). To quantify the decrease of the dye concentration, a sample of 3 ml was taken (with a pipette) at predetermined intervals of time and centrifuged at 4000 rpm.

RESULTS AND DISCUSSION

Characterization of the prepared samples

The XRD patterns of TiO_2 and doped TiO_2 samples treated at 400 °C are shown in Fig. 1. They show five primary diffractions at $2\theta = 25.3^\circ$ (100%), 38° (20 %), 48.2° (28 %) and 62.5° (10 %) which can be attributed to different planes of pure anatase form of TiO_2 [20,31]. Other diffractions at $2\theta = 27.36^\circ$ (100%), 36° (45%), 54.0° (53 %) and 69.0° (8 %) can be attributed to pure rutile form of TiO_2 [32]. The XRD patterns of the Cu/ TiO_2 samples almost coincide with that of the bare TiO_2 (P25) or TiO_2 treated at 400 °C showing no new diffractions due to copper doping thus suggesting that the small metal ion amounts are placed on the surface of the TiO_2 crystal (Fig. 1)[32]. The % of the two

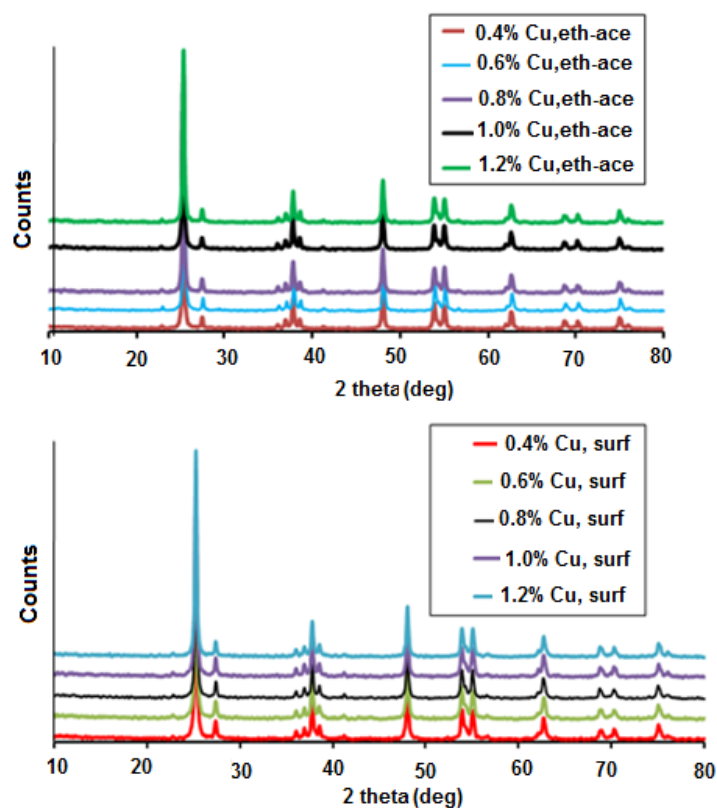


Fig. 1. The XRD patterns of the Cu/ TiO_2 samples prepared in two different media

diffractions at $2\theta = 25.3^\circ$ and 27.5° of the different samples are shown in Table 1.

The average size of the TiO_2 crystal was estimated by the Scherrer equation (Eq. 2) for all the samples [20] (Table 1):

$$D = k\lambda / (\beta \cos \theta) \quad (2)$$

Where, D represents the mean crystal dimension, λ is the X-ray wavelength (0.1541 nm), β refers to the diffraction full width at half maximum (FWHM) in radian for diffraction at $2\theta = 25.3^\circ$, K represents a

coefficient (0.89) and θ is the diffraction angle. The doped samples did not have the same crystal size as the untreated one (P25) due to agglomeration of tiny particles. The % of the ratio of rutile to anatase in P25 is 16 % whereas it varies between 8.3% and 9.6% for the samples prepared in the ethanol-acetone medium. The ratio of rutile/anatase of the two samples of TiO_2 : 0 %Cu, eth-ace and 0% Cu, surf are lower than that of the bare TiO_2 whereas the particle dimension (D) is higher in both cases (Table 1).

Fig. 2 shows the FTIR spectra of TiO_2 and Cu/ TiO_2 samples. The FTIR spectrum of TiO_2 shows

Table 1. TiO_2 crystal dimension and relative intensity of some characteristic peaks of P25 and the prepared samples, (Anatase (A), Rutile (R)).

Sample	$2\theta = 25.3^\circ$ (A)	$2\theta = 27.36^\circ$ (R)	D (nm)	% (rutile/anatase)
P25	100	16.5	23.0	16.0
0% Cu, eth-ace	100	13.2	26.8	13.0
0% Cu, surf	100	12.6	27.8	12.5
0.4 % Cu, eth-ace	100	8.0	35.0	8.3
0.4% Cu, surf	100	10.3	32.2	10.4
0.8 % Cu, eth-ace	100	8.7	32.2	9.6
0.8 % Cu, surf	100	9.4	33.6	9.6
1.2 % Cu, eth-ace	100	9.0	33.6	9.3
1.2% Cu, surf	100	8.7	32.2	9.0

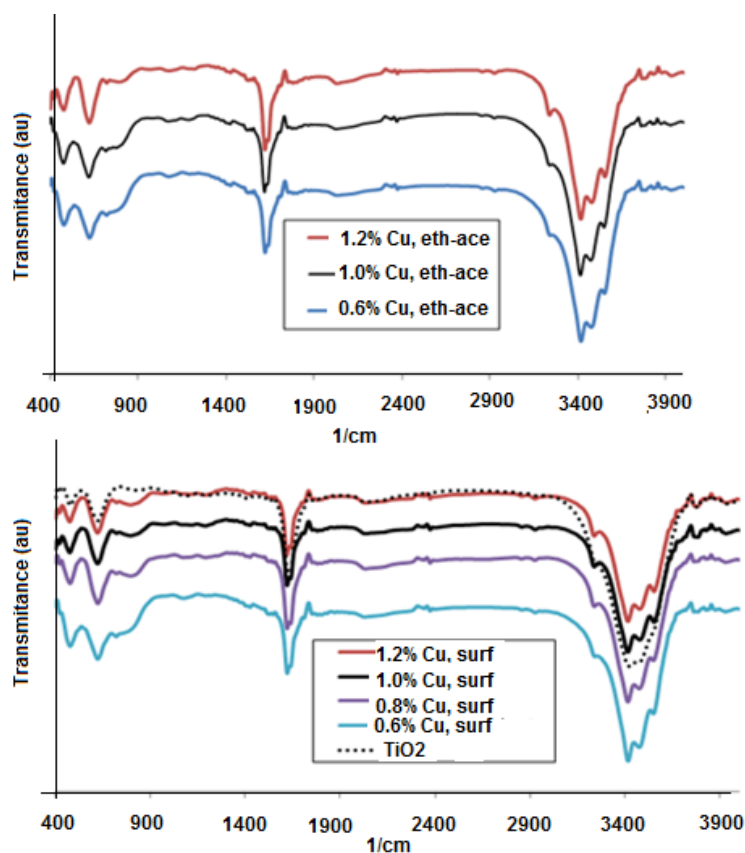


Fig. 2. FTIR spectra of TiO_2 and Cu/ TiO_2 samples prepared in two different media

three bands: broad and intense one at 3420 cm^{-1} , the two other bands at 1620 and 620 cm^{-1} . The peaks at 3420 and 1620 cm^{-1} can be attributed to the O–H stretching and bending mode of hydroxyl groups of moisture that is present on the surface of the catalyst [33, 34]. These are critical for photocatalytic reactions since they can react with photogenerated holes produced on the catalyst surface and generated hydroxyl radicals, which are powerful oxidant. The peaks of TiO_2 observe at 476 and 620 cm^{-1} can be assigned to the vibrations of Ti–O and Ti–O–Ti framework bonds of TiO_2 [33]. The zoom in the region between 400 and 600 cm^{-1} did not show any characteristic peak of Cu–O (432.3 , 497 , and 603 cm^{-1}) [35]. As the amount added of the metal salts are small, no new band and no shift is observed in the bands of the bare TiO_2 after Cu doping.

In the Raman spectrum of P25, the peaks centered at 145 , 396 , 514 and 636 cm^{-1} are attributed to the anatase phase, while the peaks, located at 245 , 443 and 610 cm^{-1} are characteristic of the rutile phase of TiO_2 (Fig. 3) [35–37]. The Raman spectra of P25 and Cu/ TiO_2 samples consisted of characteristic peaks of anatase (Fig. 3). No shift was observed after doping with 1.2% Cu(II) [38]. As in the case of XRD, the presence of copper oxide CuO or Cu_2O could not be detected by Raman spectroscopy [35]. The non-detection of the corresponding metallic oxide by these techniques (Raman, XRD, and IR)

does not mean its absence, due to the small amount of copper.

The electronic band structures of the as-prepared samples were analyzed by UV–Vis diffuse reflectance spectroscopy (Fig. 4a). All the samples exhibited reflectance in the range of 250 – 400 nm that can be attributed to anatase and rutile phase of TiO_2 . The Cu-doped sample indicated a redshift extending up to 600 nm that attributed to the presence of Cu in these samples. The successful doping of Cu was also evident from the change in the color observed in the samples, shifting from pure white to light yellow. The optical band gap energy of the prepared samples was determined by UV-Vis DRS analysis [31], and the obtained DRS results are reported as the Kubelka–Munk function where R is the reflectance, $F(R)$ is the Kubelka–Munk function (Eq. 3):

$$F(R) = (1 - R)^2 / 2R \quad (3)$$

The optical band gap energy of the samples can be derived from UV-Vis DRS data by plotting $F(R)$ against photon energy ($E: h\nu$), followed by extrapolation of the linear part of the spectra to the energy axis (Fig. 4b) [30]. The increase in the bandgap energy of the 1.0 and 1.2% Cu, surf samples (3.25 and 3.21 eV) with respect to that of P25 (3.12 eV) may be due to rutile/ anatase ratio in these samples. The rutile/anatase ratio is 9.3%

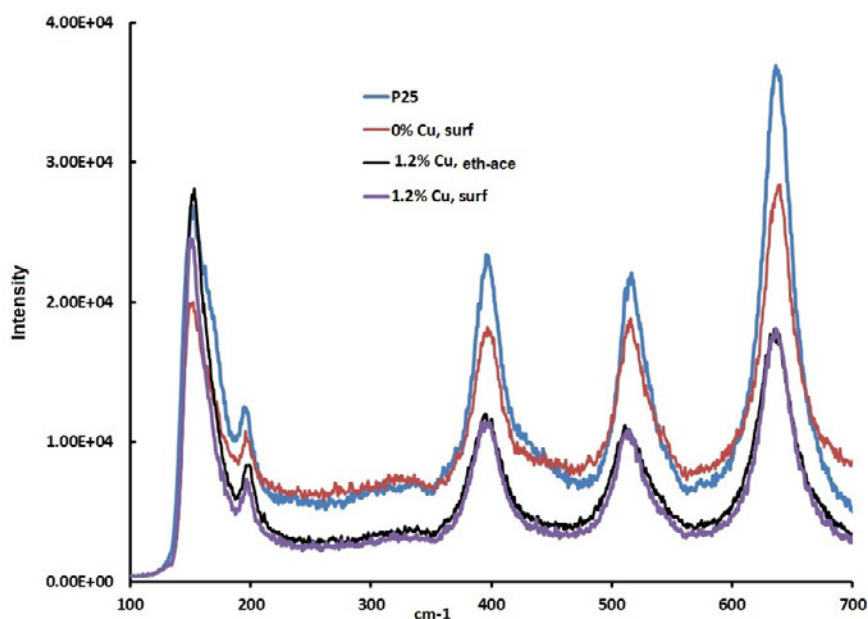


Fig. 3. Raman spectra of the samples prepared in two different media.

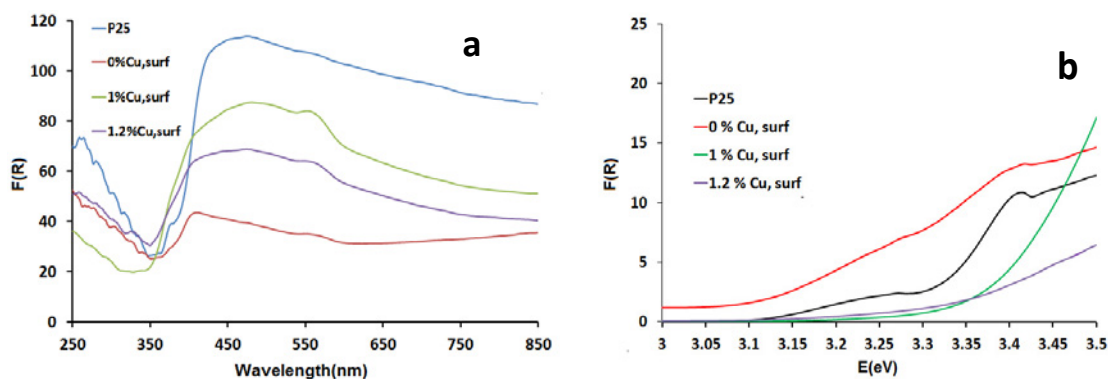


Fig. 4. a) Diffuse reflectance spectra and b) Kubelka-Munk curves of the samples for calculation of bandgap energy.

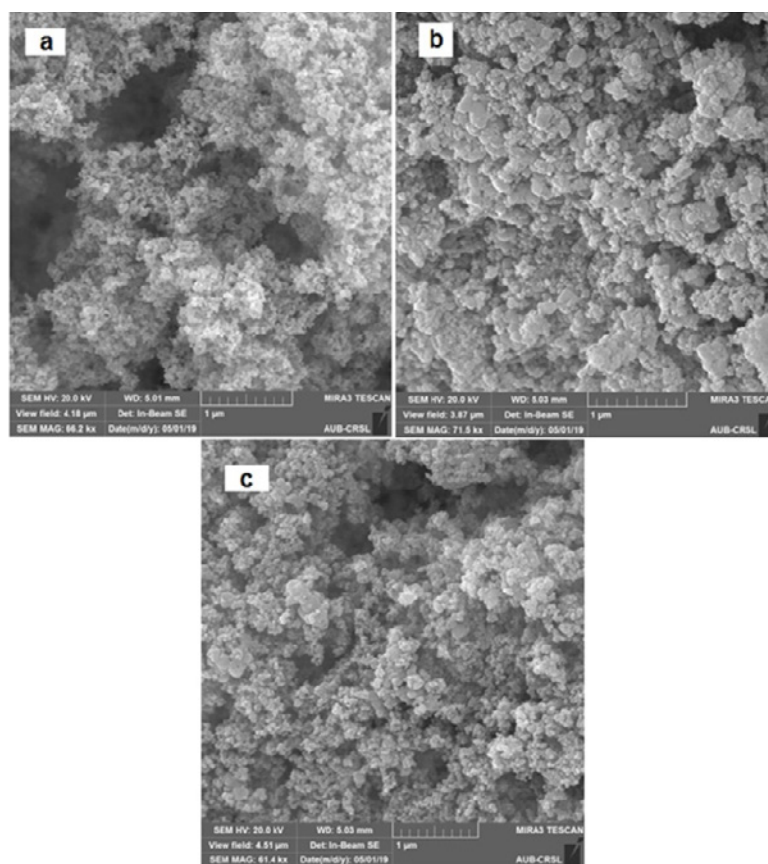


Fig. 5. SEM images of a) P25, b) 1.2 % Cu, eth-ace, c) 1.2 % Cu, surf.

and 9.0% for 1.0 and 1.2% Cu, surf samples and the bandgap energy for anatase and rutile phase of TiO₂ are 3.20 and 3.00 eV respectively. The bandgap energy of Cu doped samples shifted to bandgap energy of pure anatase phase by decreasing rutile/anatase ratio.

SEM images of the TiO₂ and 1.2 % Cu/TiO₂ samples prepared in two different media are shown in Fig. 5. SEM images show that the samples

prepared by the two procedures are agglomerated; also the particles are bigger than the bare TiO₂. The EDX patterns of Cu/TiO₂ samples (Fig. 6) show two peaks around 0.2 and 4.5 keV. The intense peak is assigned to the bulk TiO₂ and the less intense one to the surface TiO₂ [20]. The peaks of Cu are observed at 0.7, 8 and 9 keV [34]. The results confirm the existence of Cu atoms in the Cu/TiO₂ samples (Table 2), but the XRD patterns did not show any

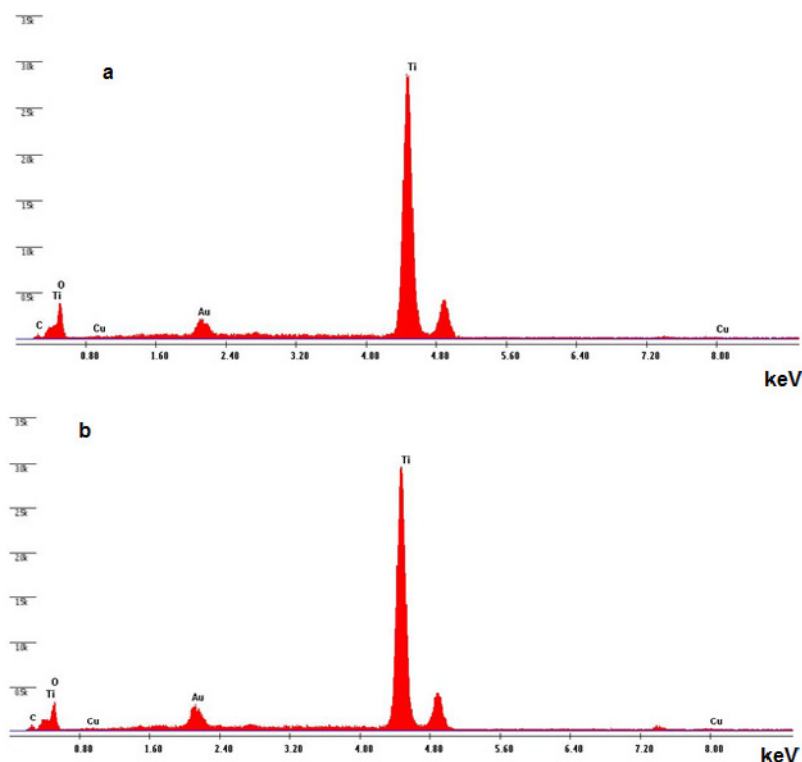


Fig. 6. EDX pattern for sample a) 1.2% Cu, eth-ace and b) 1.2% Cu, surf.

Table 2. Chemical composition of the prepared samples (At%: atomic%).

Sample	C (At%)	O (At%)	Ti (At%)	Cu (At%)
P25	5.00	50.0	45.0	-
1.2% Cu, eth-ace	35.5	43.0	21.0	0.50
1.2% Cu, surf	39.53	50.0	10.0	0.47

diffractions related to Cu. EDX analysis shows that some zones contain high atomic % of C. It may be due to organic molecules adsorbed chemically on the surface of the TiO₂ nanoparticles.

Photocatalytic activity of Cu doped TiO₂

The variation of the UV- visible spectrum of the dye versus time shows a decrease of all the spectra with time. The photocatalytic degradation of E 131 VF dye in the presence of the bare TiO₂ follows perfectly the pseudo-first-order kinetics (Fig. 7). Also the photocatalytic degradation reaction order obtained in the presence of TiO₂ with 0 % and 0.2 % Cu in the two media (calcined at 400 °C) were pseudo-first-order, but it became zero order for higher % of Cu (Fig. 7). There is a blue shift of the maximum wavelength (indicated by dotted line in Fig. 8) that proving a successive degradation of dye during irradiation. A similar result was obtained

with Baraka [40]. The time needed to decrease the absorbance from 1.6 to 0.1 for the bare P25 was 12 min whereas it was 20 min for 0% Cu, eth-ace and 28 min for 0% Cu, surf. The impregnation of TiO₂ in the acetone-ethanol and in the aqueous solution of surfactant affected the surface of TiO₂ may be by adsorption of these organic molecules at the surface of TiO₂ or by agglomeration of the nanoparticles of P25. The rate constants of TiO₂ with 0 % Cu in the two media were for the 1st procedure: 0.14 and for the 2nd one: 0.098, which are both smaller than the bare TiO₂ ($k_0=0.24$ (au)) and P25 heated at 400 °C without addition of any solvent for 4 h ($k_0=0.23$ (au)) (Fig. 9). The decrease in the activity of TiO₂ after solvation is due to increase in agglomeration of the nanoparticles of TiO₂ and maybe also due to the adsorption of organic solute (ethanol/acetone or surfactant) on the surface of TiO₂ which prevent the absorption of the radiation and therefore the

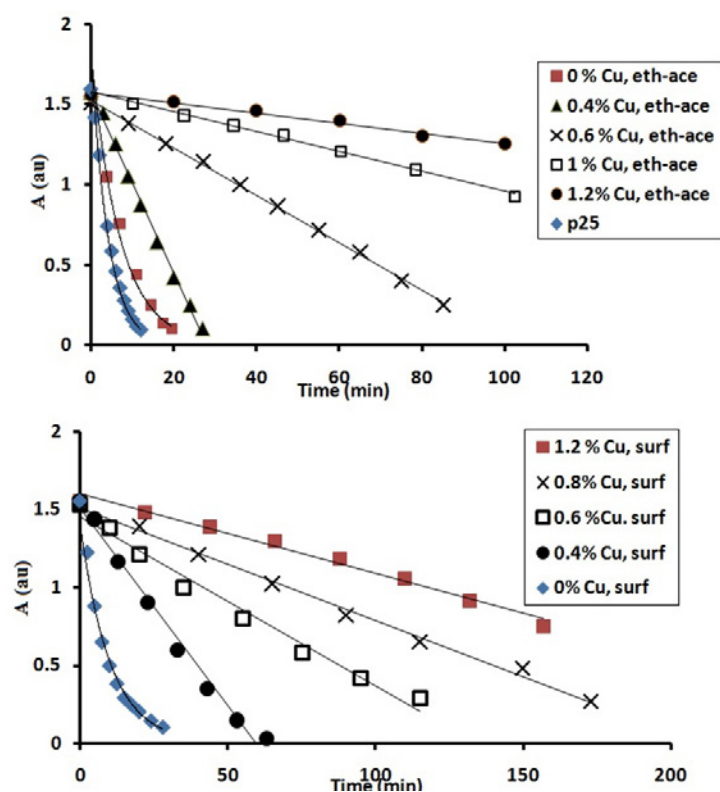


Fig. 7. Variation of the absorbance as a function of time for various Cu doped TiO₂ samples prepared in two different media.

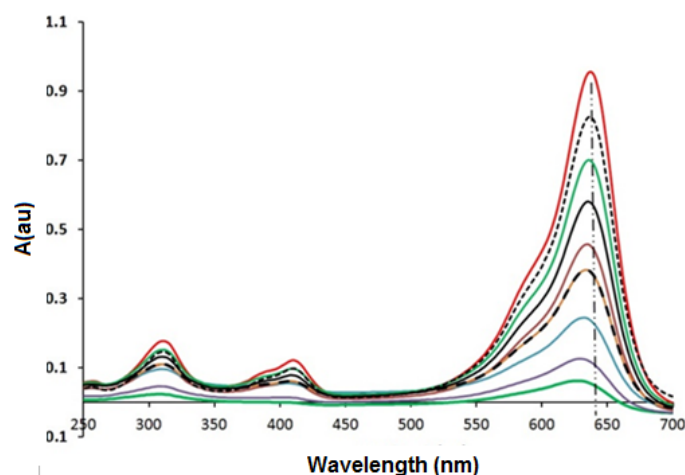


Fig. 8. Variation of the UV-Visible spectrum during the photocatalytic degradation of E 131 VF dye in the presence of P25.

good function of TiO₂. The rate constant in the acetone –ethanol medium is higher than that in the surfactant medium. For higher % of Cu the rate constant k_0 is approximately the same (Fig. 9). For all the doped samples (including 0 % Cu), the rate constant is smaller than that of P25. The results of several works show a decrease in the photoactivity after doping with Cu(II) (Table 3). There are several

factors which inhibit the photoactivity of TiO₂:

- 1) The adsorption of the organic molecules (surfactant or ethanol) on the surface of TiO₂
- 2) The agglomeration of the TiO₂ nanoparticles during solvation, so the particles of these catalysts are not well distributed in the food colorant solution as was the case with P25. The surface area available for photon absorption would be reduced.

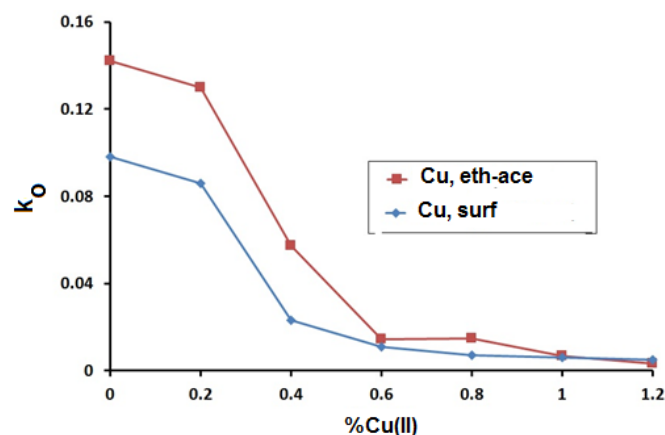


Fig. 9. Variation of the rate constant of k_o vs the Cu(II) molar ratio %.

Table 3. Effect of doping Cu(II) to TiO_2 on the photocatalytic degradation of the organic pollutants.

Pollutant	Range of doping %	Optimum % of doping	reference
Rhodamine B	0 -1	0.06	[15]
Ethanoic acid	1 (only one %)	Negative effect for any %	[23]
4-Nitrophenol	0.3 – 5.0	Negative effect for any %	[28]
Acid orange 7	1 (only one %)	Negligible effect	[24]
E 131 VF dye	0.2 -1.2	Negative effect for any %	This work

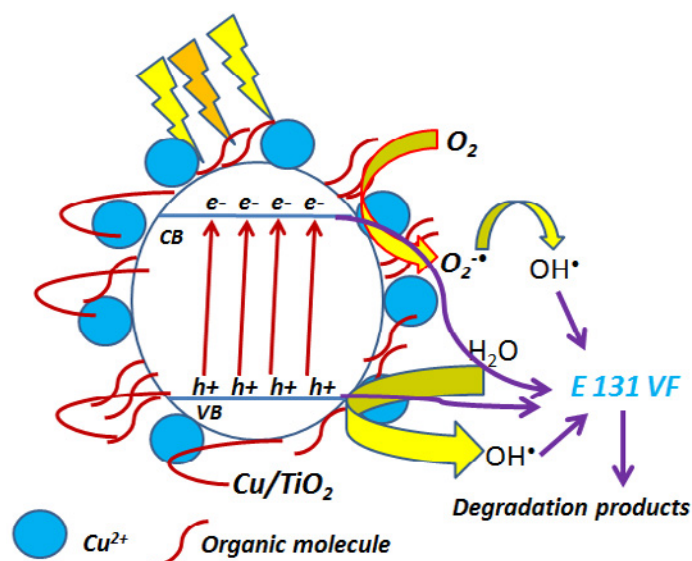


Fig.10. Our proposed mechanism for photocatalytic degradation of E 131 VF dye over Cu/TiO₂ photocatalyst under UV irradiation.

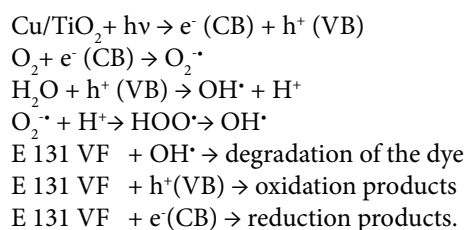
3) The increase in the recombination of photogenerated electrons and holes which is a function of the amount of Cu added. Paola et al. showed that the rate constants of e^-h^+ recombination increases when metal loading increases [22].

Proposed mechanism for E 131 VF dye degradation

Fig. 10 shows the surface of TiO_2 after doping

by Cu^{2+} in organic media and proposed mechanism for the photocatalytic degradation of E 131 VF dye over Cu/TiO₂ sample. High-energy electrons are formed on Cu/TiO₂ surface under UV irradiation. These electrons are excited from valence band to conduction band of TiO_2 and the holes remain on the valence band of TiO_2 . The oxygen molecules adsorbed on the surface of photocatalyst trap the electron from the TiO_2 and thus a number of

active species including OH^\bullet and $\text{O}_2^{\bullet-}$ radicals are produced. These species attack to E 131 VF dye molecules and decompose them. The photoinduced holes (h^+) can react with H_2O oxidizing them to OH^\bullet radicals or oxidize the dye molecules. The reactions at the surface of photocatalyst initiating the degradation of E 131 VF dye can be expressed as follows:



CONCLUSION

In this work, we prepared Cu doped TiO_2 samples containing different amounts of Cu (0.2-1.2 % mole ratio) in two different media by impregnation method. The XRD, Raman and FTIR techniques which are bulk techniques were unable to prove the presence of small amounts of copper on the surface of TiO_2 , but the EDX analysis confirmed 0.5 At% of Cu. The crystal dimension of TiO_2 increased in the range of 26-35nm but the rutile /anatase ratio decreased from 16% to 9% after Cu doping in two different media compared to P25. We used the prepared samples for kinetics study of the photocatalytic degradation of food colorant E 131 VF. Our obtained results showed that the doping TiO_2 with Cu(II) had a detrimental effect on the photocatalytic activity of TiO_2 whatever the solvent used due to agglomeration of the nanoparticles and presence of some organic molecules on TiO_2 surface. The photocatalytic degradation rate constant of TiO_2 (P25) was 0.24 (au) but it decreased to 0.015 (au) in the presence of the sample containing 0.6% Cu. We suggest studying the effect of doping to add the metal salt during the sol gel preparation of TiO_2 in order to prevent the agglomeration of the nanoparticles.

ACKNOWLEDGEMENT

The author thanks the Lebanese University for providing financial assistance to carry out this work.

CONFLICTS OF INTEREST

There are no conflicts to declare.

REFERENCES

1. Fonovich TM. Sudan dyes: are they dangerous for human health? *Drug and Chemical Toxicology*. 2012;36(3):343-52.
2. Inetianbor, J. E., Yakubu, J. M. and Ezeonu, S. C.: Effect of food additives and preservatives on man, a review. *Asian J. Sci. Technol.* 6(2), 118–1124(2015)
3. Roy DC, Biswas SK, Saha AK, Sikdar B, Rahman M, Roy AK, et al. Biodegradation of Crystal Violet dye by bacteria isolated from textile industry effluents. *PeerJ*. 2018;6:e5015.
4. Tabarra, M.A., Mallah, H. A., El Jamal, M. M.: Anodic oxidation of anionic xanthene dyes at Pt and BDD electrodes. *J. Chem. Technol. Metall.* 49(3), 247–253 (2014)
5. Mallah HA, Naoufal DM, Safa AI, El-Jamal MM. Study of the Discoloration Rate of Rhodamine B as a Function of the Operating Parameters at Pt and BDD Electrodes. *Portugaliae Electrochimica Acta*. 2013;31(3):185-93.
6. El Jamal, M.M., Ncibi, M.C.: Biosorption of methylene blue by chaetophora elegans algae: Kinetics, equilibrium and thermodynamic studies. *Acta Chim. Slov.* 59(1) 24–31 (2012)
7. Vaiano V, Iervolino G, Rizzo L, Sannino D. Advanced Oxidation Processes for the Removal of Food Dyes in Wastewater. *Current Organic Chemistry*. 2017;21(12):1068-73.
8. Naser Elddine HA, Damaj ZK, Yazbeck OA, Tabbara MA, El-Jamal MM. Kinetic Study of the Discoloration of the Food Colorant E131 by $\text{K}_2\text{S}_2\text{O}_8$ and KIO_3 . *Portugaliae Electrochimica Acta*. 2015;33(5):275-88.
9. Saquib M, Abu Tariq M, Faisal M, Muneer M. Photocatalytic degradation of two selected dye derivatives in aqueous suspensions of titanium dioxide. *Desalination*. 2008;219(1-3):301-11.
10. Chen C-C, Lu C-S, Mai F-D, Weng C-S. Photooxidative N-de-ethylation of anionic triarylmethane dye (sulfan blue) in titanium dioxide dispersions under UV irradiation. *Journal of Hazardous Materials*. 2006;137(3):1600-7.
11. Diao Z-H, Xu X-R, Liu F-M, Sun Y-X, Zhang Z-W, Sun K-F, et al. Photocatalytic degradation of malachite green by pyrite and its synergism with Cr(VI) reduction: Performance and reaction mechanism. *Separation and Purification Technology*. 2015;154:168-75.
12. Samsudin EM, Sze NG, Ta YW, Tan TL, Abd. Hamid SB, Joon CJ. Evaluation on the Photocatalytic Degradation Activity of Reactive Blue 4 using Pure Anatase Nano- TiO_2 . *Sains Malaysiana*. 2015;44(7):1011-9.
13. Akpan UG, Hameed BH. Parameters affecting the photocatalytic degradation of dyes using TiO_2 -based photocatalysts: A review. *Journal of Hazardous Materials*. 2009;170(2-3):520-9.
14. Tayade RJ, Kulkarni RG, Jasra RV. Transition Metal Ion Impregnated Mesoporous TiO_2 for Photocatalytic Degradation of Organic Contaminants in Water. *Industrial & Engineering Chemistry Research*. 2006;45(15):5231-8.
15. Xin B, Wang P, Ding D, Liu J, Ren Z, Fu H. Effect of surface species on Cu- TiO_2 photocatalytic activity. *Applied Surface Science*. 2008;254(9):2569-74.
16. Liao DL, Badour CA, Liao BQ. Preparation of nanosized TiO_2/ZnO composite catalyst and its photocatalytic activity for degradation of methyl orange. *Journal of Photochemistry and Photobiology A: Chemistry*. 2008;194(1):11-9.
17. Filippo E, Carlucci C, Capodilupo AL, Perulli P, Conciauro F, Corrente GA, et al. Enhanced Photocatalytic Activity of Pure Anatase TiO_2 and Pt- TiO_2 Nanoparticles Synthesized

- by Green Microwave Assisted Route. *Materials Research*. 2015;18(3):473-81.
18. Gupta AK, Pal A, Sahoo C. Photocatalytic degradation of a mixture of Crystal Violet (Basic Violet 3) and Methyl Red dye in aqueous suspensions using Ag⁺ doped TiO₂. *Dyes and Pigments*. 2006;69(3):224-32.
19. Mahmoud, G.E.A., Ismail, L.F.M.: Photocatalytic degradation of Direct Yellow 50 on TiO₂. *J Am Sci*. 8(10), 83–99 (2012)
20. Pirbazari AE, Monazzam P, Kisomi BF. Co/TiO₂ nanoparticles: preparation, characterization and its application for photocatalytic degradation of methylene blue. *DESALINATION AND WATER TREATMENT*. 2017;283-92.
21. Khairy M, Zakaria W. Effect of metal-doping of TiO₂ nanoparticles on their photocatalytic activities toward removal of organic dyes. *Egyptian Journal of Petroleum*. 2014;23(4):419-26.
22. Begum, T., Gogoi, P.K., Bora, U.: Photocatalytic degradation of crystal violet dye on the surface of Au doped TiO₂ nanoparticles. *INDIAN J. CHEM. TECHNOL.* **24**, 97–101 (2017)
23. Di Paola A, Garcí'a-López E, Ikeda S, Marci' G, Ohtani B, Palmisano L. Photocatalytic degradation of organic compounds in aqueous systems by transition metal doped polycrystalline TiO₂. *Catalysis Today*. 2002;75(1-4):87-93.
24. Rao KVS, Lavédrine B, Boule P. Influence of metallic species on TiO₂ for the photocatalytic degradation of dyes and dye intermediates. *Journal of Photochemistry and Photobiology A: Chemistry*. 2003;154(2-3):189-93.
25. Riaz N, Mohamad Azmi B-K, Mohd Shariff A. Iron Doped TiO₂ Photocatalysts for Environmental Applications: Fundamentals and Progress. *Advanced Materials Research*. 2014;925:689-93.
26. Bouras P, Stathatos E, Lianos P. Pure versus metal-ion-doped nanocrystalline titania for photocatalysis. *Applied Catalysis B: Environmental*. 2007;73(1-2):51-9.
27. Elsalamony, R., El-Hafiza, D.A.: Influence of Preparation Method on Copper Loaded Titania Nanoparticles: Textural, Structural Properties and Its Photocatalytic Activity towards P-Nitrophenol. *Chem. and Materials Res.* **6**(4), 122–134 (2014)
28. Di Paola A, Marci G, Palmisano L, Schiavello M, Uosaki K, Ikeda S, et al. Preparation of Polycrystalline TiO₂ Photocatalysts Impregnated with Various Transition Metal Ions: Characterization and Photocatalytic Activity for the Degradation of 4-Nitrophenol. *The Journal of Physical Chemistry B*. 2002;106(3):637-45.
29. El Jamal, M.M, Estephane, G.C.: Effect of Doping of TiO₂ nanoparticles with Silver on their Photocatalytic Activities toward Degradation of E 131 VF. Accepted recently in *J. Chem. Technol. Metall.* **54** (5), 926-933 (2019).
30. Mahyar A, Amani-Ghadim AR. Influence of solvent type on the characteristics and photocatalytic activity of TiO₂ nanoparticles prepared by the sol–gel method. *Micro & Nano Letters*. 2011;6(4):244.
31. Anku W, Osei-Bonsu Oppong S, Kumar Shukla S, Penny Govender P. Comparative photocatalytic degradation of monoazo and diazo dyes under simulated visible light using Fe³⁺/C/S doped-TiO₂ nanoparticles. *Acta Chimica Slovenica*. 2016:380-91.
32. Ijadpanah-Saravy H, Safari M, Khodadadi-Darban A, Rezaei A. Synthesis of Titanium Dioxide Nanoparticles for Photocatalytic Degradation of Cyanide in Wastewater. *Analytical Letters*. 2014;47(10):1772-82.
33. Elsalamony, R., El-Hafiza, D.A.: Influence of Preparation Method on Copper Loaded Titania Nanoparticles: Textural, Structural Properties and Its Photocatalytic Activity towards P-Nitrophenol. **6**(4), 122–134 (2014)
34. Ghasemi S, Rahimnejad S, Setayesh SR, Rohani S, Gholami MR. Transition metal ions effect on the properties and photocatalytic activity of nanocrystalline TiO₂ prepared in an ionic liquid. *Journal of Hazardous Materials*. 2009;172(2-3):1573-8.
35. Ethiraj AS, Kang DJ. Synthesis and characterization of CuO nanowires by a simple wet chemical method. *Nanoscale Research Letters*. 2012;7(1).
36. Tasbihi M, Kočí K, Troppová I, Edelmánová M, Reli M, Čapek L, et al. Photocatalytic reduction of carbon dioxide over Cu/TiO₂ photocatalysts. *Environmental Science and Pollution Research*. 2017;25(35):34903-11.
37. Wypych A, Bobowska I, Tracz M, Opasinska A, Kadlubowski S, Krzywania-Kaliszewska A, et al. Dielectric Properties and Characterisation of Titanium Dioxide Obtained by Different Chemistry Methods. *Journal of Nanomaterials*. 2014;2014:1-9.
38. Choudhury B, Dey M, Choudhury A. Defect generation, d-d transition, and band gap reduction in Cu-doped TiO₂ nanoparticles. *International Nano Letters*. 2013;3(1).
39. Nguyen VN, Nguyen NKT, Nguyen PH. Hydrothermal synthesis of Fe-doped TiO₂ nanostructure photocatalyst. *Advances in Natural Sciences: Nanoscience and Nanotechnology*. 2011;2(3):035014.
40. Barka N, Qourzal S, Assabbane A, Nounah A, Ait-Ichou Y. Photocatalytic Degradation of Patent Blue V by Supported TiO₂: Kinetics, Mineralization, and Reaction Pathway. *Chemical Engineering Communications*. 2011;198(10):1233-43.